International Journal of Robotics and Control Systems
Vol. 5, No. 6, 2025, pp. 2709-2728
ISSN 2775-2658
http://pubs2.ascee.org/index.php/ijrcs

Enhanced DC-Link Voltage Stability in Grid-Connected PV Systems via Three Recent Metaheuristic Optimizers: Towards High Penetration of PV Systems in modern power systems

Mohammed M. Alrashed [a,1], Mohamed F. Elnaggar [a,2,*]

[a] Department of Electrical Engineering, College of Engineering, Prince Sattam Bin Abdulaziz University, Al-Kharj 11942, Saudi Arabia
[1] mm.alrashed@psau.edu.sa; [2] mfelnaggar@yahoo.com
* Corresponding Author

ARTICLE INFO

Article history
Received September 19, 2025
Revised October 28, 2025
Accepted November 26, 2025

Keywords
Sustainable Development;
Optimization Methods;
Grid Integration;
DC Bus Voltage Stability;
Solar Energy Control

ABSTRACT

As more grid-connected PV units are being installed, it is becoming challenging to sustain DC bus voltage stability (DCBVS). Since optimization techniques are frequently employed to improve the control process, they are ideally adapted to the dynamic operating conditions of systems that are integrated with renewable energy. The goal of this research is to improve DCBVS in networked PV systems by optimizing PI controllers using the GRO method. The study emphasizes how important DCVS is to sustaining network dependability and legal compliance under different faults. Using important dynamic response parameters including OS, ST, and SSE, the accuracy of GRO is assessed in conjunction with that of PSO and the WOA in order to assess its efficacy. The GRO-based controller reduces VDC-OS by 4.75% when compared to PSO and by 2.85% when compared to WOA in a 3L-G fault. In addition, GRO has the quickest ST action, cutting the time by 2.75% when compared to PSO and WHO. When it comes to SSE accuracy, GRO has the smallest % inaccuracy. In total, the findings show that the GRO provides a useful approach for stabilizing the VDC under harsh faults.

1. Introduction

Emissions of greenhouse gases, particularly CO_2 from FFs, have been a major contributor to the recent decades' rapid climate change [1], [2]. The energy mix must shift from FFs to RESs including PV, biofuels, hydropower, geothermal, and wind in order to reduce these emissions [3], [4]. PV systems must fulfill strict reliability requirements, guaranteeing that every component operates as intended, in order to be practical and economical [5]. However, design flaws and environmental factors can lead to PV system failures, especially with regard to their power electronics [6]-[8].

Over the years, the primary goal of GC- PV inverters have been to maximize the power output of PV modules. However, by providing extra ancillary services, they can also help maintain grid stability [9], [10]. According to international regulations, new PV inverters are now expected to provide these auxiliary capabilities in order to preserve the stability and integrity of the power supply. These functions aid in reestablishing equilibrium when load and generation are out of balance [11]-

[13]. Future PV inverters will have increased power density, efficiency, and dependability due to continuous technical advancements. Although it helps the power system fulfill growing energy demands, integrating RESs poses stability issues [14], [15]. Operators constantly update grid codes and standards in order to adapt. The impact of grid failures on interconnected RESs installations is a major worry. This is addressed by FRT standards, which guarantee that renewable units continue to function during brief voltage drops, preserving system stability in the event of a malfunction [16]-[18].

Because three-phase transmission failures frequently resulted in total voltage decreases and decreased power output, wind turbines were historically the main focus of FRT regulations [19]-[21]. However, in order to prevent complete power loss and guarantee system dependability, FRT requirements for PV systems have become equally crucial due to the increasing proliferation of PV power plants. In order to ensure transient stability and post-fault synchronization, FRT capability—which is evaluated in labs using specialist units—is essential for preserving converter operation during brief grid outages [22], [23].

FRT augmentation in GC- PV systems have been the subject of numerous studies. approaches include advanced control systems for managing active and reactive power [24], [25], current control approaches to reinforce fault performance [26], and adaptive power tracking for increased efficiency without additional hardware [20]. Other papers focus on instantaneous power theory for optimal fault response [27], flexible current control algorithms [28], and active power curtailment [29]. Fuzzy logic [30], [31], optimum algorithms [32], and hybrid neuro-fuzzy techniques [33] are examples of intelligent and optimal control strategies that have further improved FRT capabilities, enhancing system stability and dynamic response [34], [35].

A key element of control systems, the PI controller is frequently employed in feedback-based methods to control system output by reducing the discrepancy between desired and actual values [36]. Because of its simplicity, affordability, and convenience of use, the PI controller supports grid stability and power quality by efficiently enhancing the FRT capabilities of systems by controlling inverter voltage and current during faults [37]. GC-PV systems' transient response is further enhanced by algorithmic optimization, which lowers rising time, undershoot, and overshoot. Numerous power system issues, such as optimal power flow, reactive power and economical dispatch, and optimal allocation of FACTS, have been successfully solved by metaheuristic algorithms like PSO, WHO, HAS, POA, and GA [38]-[40].

The optimization-based improvement of FRT in PV systems has been the subject of numerous studies. In [41], PI controllers in multi-area power systems were tuned using BFO and PSO. PSO had subpar FRT performance and premature convergence, despite achieving effective tuning. Likewise, [42], [43], optimized PI controllers for FRT enhancement in GC-PV systems using the MPA. Despite improvements in overshoot and settling time, comparisons with GWO and PSO revealed that both approaches lacked computational efficiency and robustness under a variety of fault circumstances.

The convergence speed, stability, and performance of conventional algorithms like PSO, GWO, and WOA under various fault scenarios continue to be issues despite a great deal of effort in this field. This work suggests GRO for PI controller tuning for DCBVS in GC- PV systems. System stability is increased during both symmetrical and asymmetrical faults thanks to the GRO approach's quicker convergence, increased precision, and better balance between transient and steady-state performance.

The structure of the paper is as follows: The GC- PV system and its control approach are explained in Section 2, the applied methods (PSO, WHO, and the proposed GRO) is presented and their cost objective function at 100 iterations in Section 3, system performance is examined under various fault scenarios in Section 4, GRO is contrasted with other optimization strategies in terms of ST, OS, and PE in Section 5, and the study is concluded in Section 6.

2. Studied System and Its Control Schemes

In order to represent electrical circuits, PV cells are connected in series or parallel to form PV arrays. The SDM is popular because it accurately and simply depicts a PV module. It has two resistances (series and parallel) to compensate for power losses, a diode, and a current source. As seen in Fig. 1, the I-V relationship is represented by a nonlinear equation, and the diode's I-V characteristics are similar to those of PV cells [44]-[46]. In [47], [48], the equations, for the real and nominal conditions are given and fully detailed.

$$I = I_{PV} - I_D - I_P \tag{1}$$

$$I_D = I_{sD}\left[e^{\left(\frac{V_D}{\alpha V_t}\right)} - 1\right] \tag{2}$$

$$V_D = V + R_S I \tag{3}$$

$$V_t = \frac{kT}{q} \tag{4}$$

$$I = I_{PV} - I_{sD}\left[e^{\left(\frac{V+R_S I}{\alpha V_t}\right)} - 1\right] - \frac{V + R_S I}{R_P} \tag{5}$$

$$I = I_{PV} - I_{D1} - I_{D2} - I_P$$
$$I = I_{PV} - I_{sD1}\left[e^{\left(\frac{V+R_S I}{\alpha_1 V_t}\right)} - 1\right] - I_{sD2}\left[e^{\left(\frac{V+R_S I}{\alpha_2 V_t}\right)} - 1\right] - \frac{V + R_S I}{R_P} \tag{6}$$

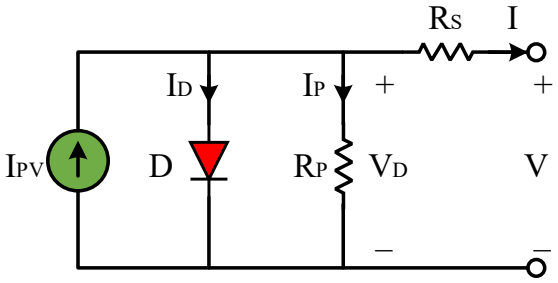

Fig. 1. SDM circuit

In the planned 100 kW system, a SunPower SPR-305E-WHT-D PV module was used. Table 1 lists its electrical properties under typical test settings and contains comprehensive details about the PV array [49]. As seen in Fig. 2, the studied system, which is modeled in MATLAB/Simulink, consists of a PV array, DC–DC converter, grid-side inverter, step-up transformer, capacitor, and a double transmission line that is connected to the grid.

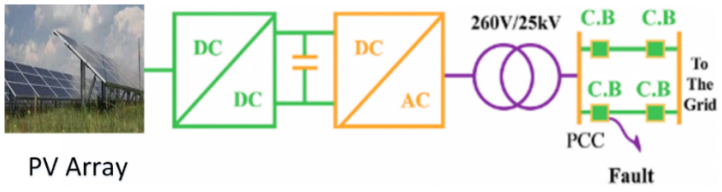

Fig. 2. Block diagram of the investigated GC-PV system

As illustrated in Fig. 3, the suggested GRO-PI controller uses the INC approach to adjust the D of the boast converter in order to accomplish MPPT [50]. For modulation, its output is contrasted with a 5 kHz TC.

Table 1. The PV array's detailed information and electrical characteristics under standard test conditions

Parameters of manufacturer	Values	Parameters of 100 kW	Vaues
P_{MAX} (W)	305.226	V_{MP} (V)	273.5
I_{SC} (A)	5.96	I_{MP} (A)	368.28
K_T (A/^{O}C)	0.061745	P_{MAX} (W)	100.35
V_{OC} (V)	64.2	N_{Series}	5
V_{MP} (V)	54.7	$N_{Parralel}$	66
K_V (mV/^{O}C)	-272.69	———	———
I_{MP} (A)	5.58	———	———

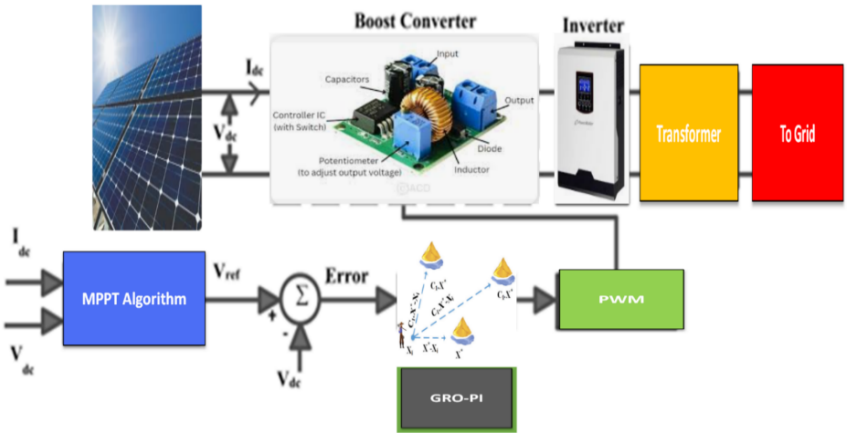

Fig. 3. Control of converter to get MPPT with the support of GRO-PI controller

The suggested solution uses an inverter with 3Ø of 6 IGBT transistors to use the GRO. Two cascaded PI loops are used to achieve the ideal PI settings, as illustrated in Fig. 4. The approach works in the rotating d-q frame, where the 3Ø -Vs and Is of the system are synchronized by a PLL. All of I_{d-q} are controlled by the inner loops, while the outer loops govern the PCC- V and the DCV, which is kept at 1 pu. Firing pulses are produced by comparing 3Ø – standard Vs obtained from d-q signals with a 5 kHz -TC The control objectives are efficiently met by the GRO- PI controllers.

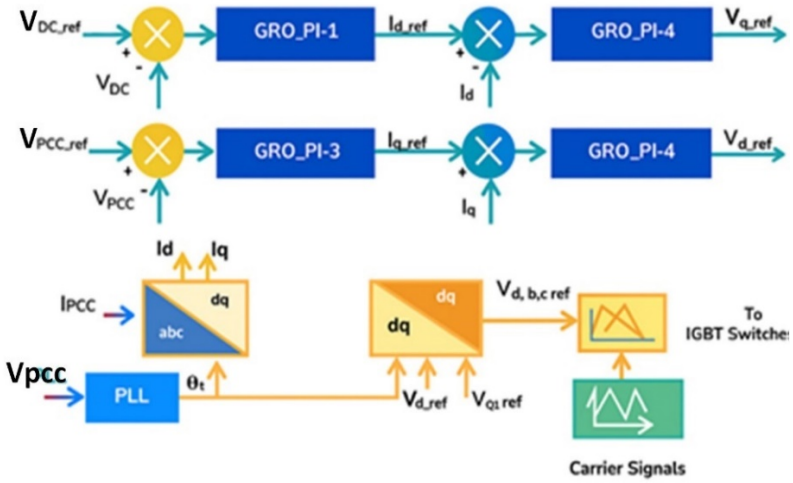

Fig. 4. System control loops based on GRO-PI controller

A GC-PV system comprising five optimized PI controllers is proposed. Two controllers (PI1, PI2) regulate the VDC, two (PI3, PI4) manage the I_d and I_q, and one (PI5) controls the PV system's INC. The GRO, WOA, and PSO optimize all (K_p and K_i). Each run 7 times with 20 iterations and 30 particles to minimize the ISE. The best fitness and objective values are presented, and GRO results are compared with PSO and WOA. The corresponding optimal PI gains are listed in Table 2.

Table 2. Optimized controller gains

Gains	PSO	WHO	GRO (proposed)
K_p1	6.218348	3.51834	4.06872
K_i1	10.21328	8.57465	12.8991
K_p2	0.034498	0.11410	0.13203
K_i2	5.988741	6.14867	7.96143
K_p3	97.18342	97.8743	98.6916
K_i3	10.03782	7.05084	7.68009
K_p4	0.088431	0.06152	0.07513
K_i4	6.809107	4.91093	6.69869
K_p5	0.181754	0.24186	0.32095
K_i5	9.240097	9.09189	8.30469

3. Implemented Optimization Techniques

3.1. PSO Method

By simulating a PS's collective behavior, the PSO effectively optimizes complicated problems. Based on its own and its neighbors' experiences, each particle iteratively changes its position and velocity, as seen in Fig. 5 [16], [51]. Convergence toward the ideal solution is made possible by PSO, which balances exploration and exploitation through velocity adjustments. The update procedure adheres to the formulas provided in [52], [53]. The symbols of equations are fully detailed in [54], [55].

$$V_i(t+1) = wv_i(t) + c_1r_1[x^*{}_i(t) - x_i(t)] + c_2r_2[g(t) - x_i(t)] \quad (7)$$

$$x_i(t+1) = x_i(t) + v_i(t+1) \quad (8)$$

3.2. WHO Method

The WHO is a metaheuristic inspired by WH' cooperative hunting behavior, used to solve complex optimization problems. Fig. 6 presents its flowchart [56]. In WOA, each whale updates its position through mathematical models that emulate encircling, spiral bubble-net, and search actions, effectively balancing exploration and exploitation. The position updates follow the equations given in [57], [58]. The next equations are fully illustrated in [56], [59].

$$\mathrm{A} = 2\mathrm{ar} - \mathrm{a} \quad (9)$$

$$\mathrm{C} = 2\mathrm{r} \quad (10)$$

$$\mathrm{X}(\mathrm{t}+1) = \mathrm{X}^*(\mathrm{t}) - \mathrm{AD} \quad (11)$$

$$\mathrm{D} = |\mathrm{C}\,\mathrm{X}^*(\mathrm{t}) - \mathrm{X}(\mathrm{t})| \quad (12)$$

$$\sum \mathrm{X}(\mathrm{t}+1) = \mathrm{X}_{\mathrm{rand}} - \mathrm{AD} \quad (13)$$

$$\mathrm{X}'(\mathrm{t}+1) = \mathrm{D}'\mathrm{e}^{\mathrm{bl}}\cos(2\pi\mathrm{l}) + \mathrm{X}^*(\mathrm{t}) \quad (14)$$

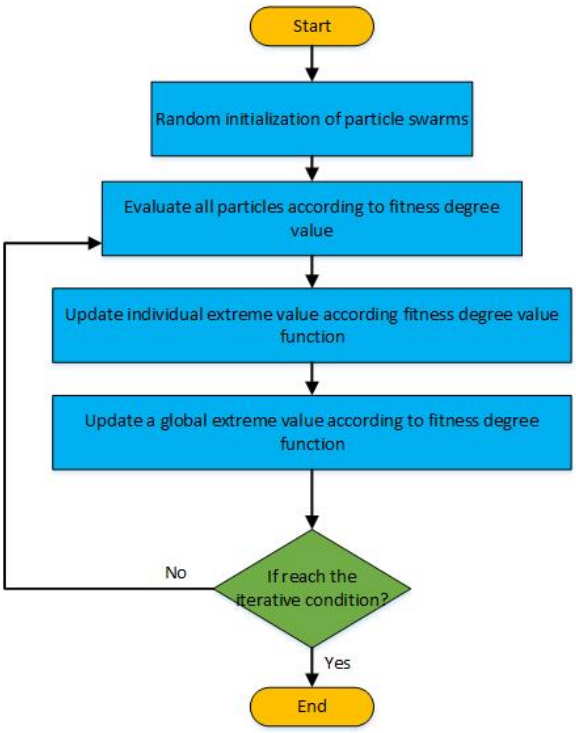

Fig. 5. PSO technique

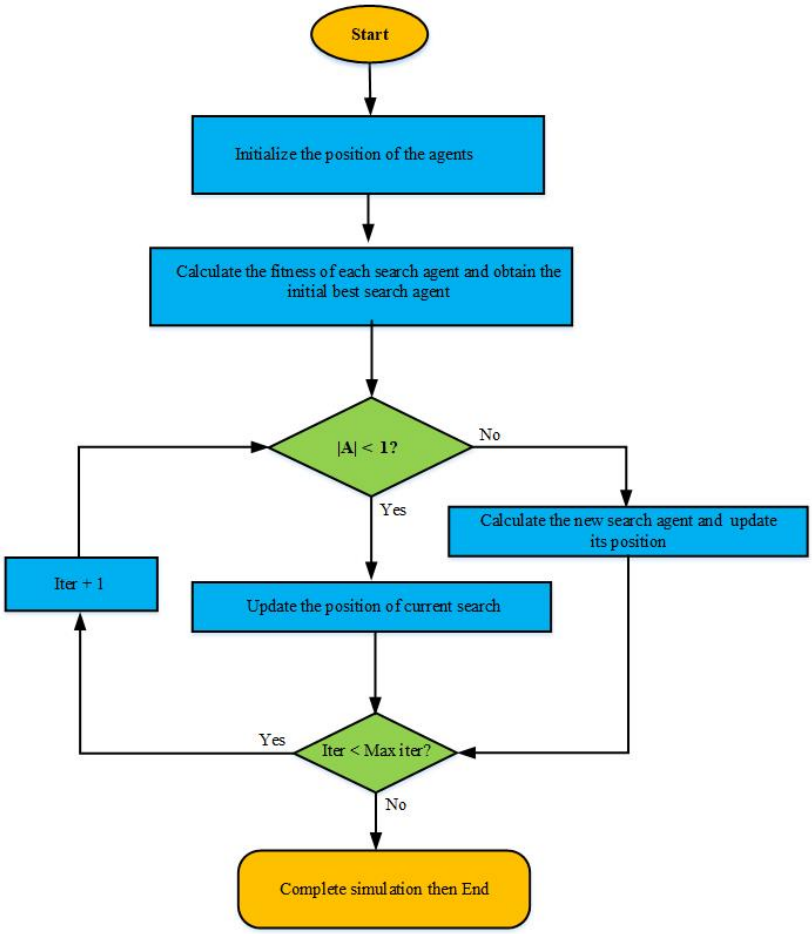

Fig. 6. WHO method

3.3. GRO Method (Proposed)

This section introduces the GRO, a population-based metaheuristic inspired by gold-seeking behaviors during the GR Era. The algorithm is founded on three main principles: migration, collaboration, and panning. After outlining their mathematical formulation, the GRO process is described in detail [60]-[63].

The GRO simulates key events of the GR. The positions of gold prospectors are stored in a matrix MGP (15), where y_{ij}denotes the position of prospector i in dimension j, and d and n represent the problem dimension and number of prospectors, respectively [64].

$$M_{GP} = \begin{bmatrix} x_{11} & x_{12} & \dots & x_{1d} \\ x_{21} & x_{22} & \dots & x_{2d} \\ \vdots & \vdots & \ddots & \vdots \\ x_{n1} & x_{n2} & \dots & x_{nd} \end{bmatrix} \tag{15}$$

An objective function evaluates each prospector's performance, with the results recorded in the MFmatrix (16). Here, y_{ij}represents the prospector's position in dimension j, and f is the evaluation function.

$$M_F = \begin{bmatrix} f(x_{11} & x_{12} & \dots & x_{1d}) \\ f(x_{21} & x_{22} & \dots & x_{2d}) \\ \vdots & \vdots & \ddots & \vdots \\ f(x_{n1} & x_{n2} & \dots & x_{nd}) \end{bmatrix} \tag{16}$$

To find GR, GR prospectors set out on expeditions. The richest gold mine in the optimization framework is the optimal location in the search space. The position of the top-performing prospector is used as a rough approximation because the precise location is unknown. The next equations are used to model the prospector's journey toward the gold mine [64].

$$\overrightarrow{D_1} = \overrightarrow{C_1}.\ \overrightarrow{X_t^*}(t) - \overrightarrow{X_t}(t) \tag{17}$$

$$\overrightarrow{Xnew_t}(t+1) = \overrightarrow{X_t}(t) + \overrightarrow{A_1}.\overrightarrow{D_1} \tag{18}$$

$$\overrightarrow{A_1} = 1 + l_1(\overrightarrow{r_1} - \frac{1}{2}) \tag{19}$$

$$\overrightarrow{C_1} = 2\,\overrightarrow{r_2} \tag{20}$$

$$l_e = \left(\frac{max_{iter} - iter}{max_{iter} - 1}\right)^e \left(2 - \frac{1}{max_{iter}}\right) + \frac{1}{max_{iter}} \tag{21}$$

Every GR prospector looks for attractive locations, and in the algebraic model, each site is a possible gold mine. The next equations are the definitions of the important mathematical relations of GR mining [64], [65]:

$$\overrightarrow{D_2} = \overrightarrow{X_t}(t) - \overrightarrow{X_r}(t) \tag{22}$$

$$\overrightarrow{Xnew_t}(t+1) = \overrightarrow{X_r}(t) + \overrightarrow{A_2}.\overrightarrow{D_2} \tag{23}$$

$$\overrightarrow{A_2} = 2l_2\,\overrightarrow{r_1} - l_2 \tag{24}$$

The collaboration between GR hunters is described in the next equations, where g1 and g2 stand for two prospectors chosen at random [64].

$$\overrightarrow{D_3} = \overrightarrow{X_{g_2}}(t) - \overrightarrow{X_{g_1}}(t) \tag{25}$$

$$\overrightarrow{Xnew_i}\,(t+1) = \overrightarrow{X_i}(t) + \overrightarrow{r_1}\,.\,\overrightarrow{D_3} \tag{26}$$

As stated in (27) for eradication instances, the GR panner goes to the fresh location if the goal function rises; if not, it stays in place. The GRO approach is illustrated in Fig. 7, highlighting its ease of use and lucidity [60].

$$\overrightarrow{X_i}(t+1) = \overrightarrow{Xnew_i}\,(t+1) \qquad \text{if } f\left(\overrightarrow{Xnew_i}\,(t+1)\right) < f\left(\overrightarrow{X_i}(t)\right) \tag{27}$$

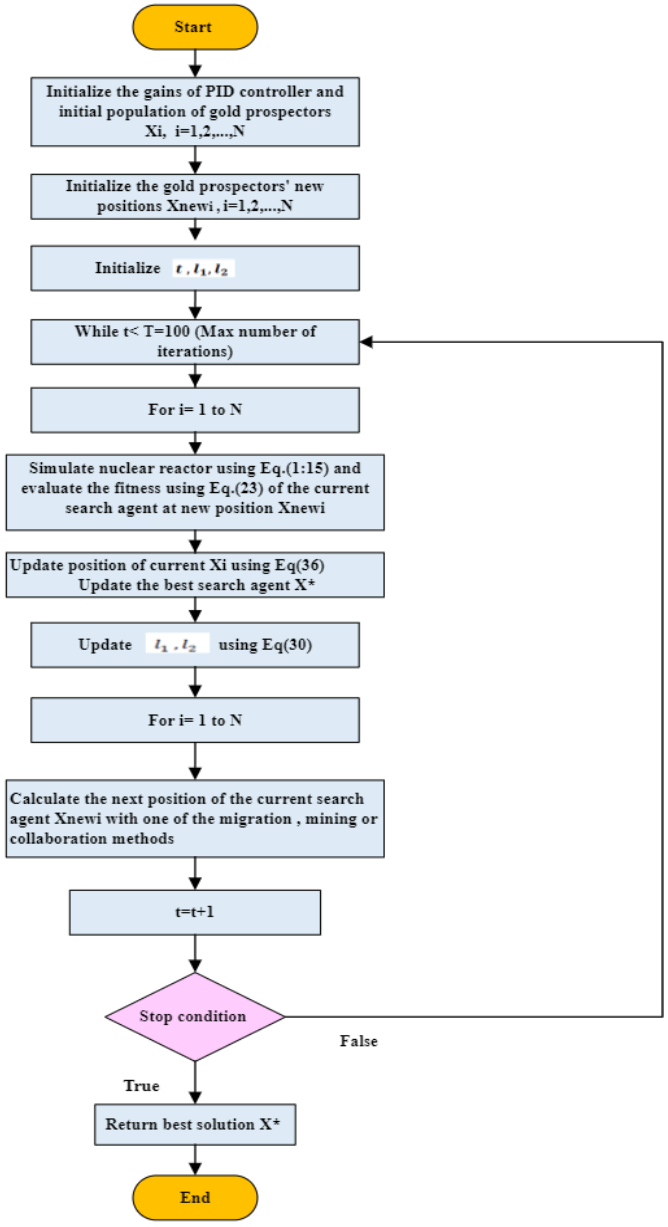

Fig. 7. GRO flowchart [64]

Fig. 8 illustrates the convergence characteristics of three optimization algorithms— PSO, WHO, and the proposed GRO—in minimizing the cost function over 100 iterations. The x-axis represents the number of iterations, while the y-axis (logarithmic scale) shows the corresponding cost function values. From the graph, the GRO demonstrates the fastest and most consistent convergence, achieving the lowest cost value among the three algorithms. This indicates that GRO provides superior optimization efficiency and stability, reaching an optimal solution with fewer iterations. In contrast, the PSO shows slower convergence and higher final cost values, suggesting it gets trapped in local minima. The WHO performs better than PSO but still converges to a higher cost than GRO. Overall, the GRO exhibits the best optimization performance, achieving a more accurate and stable solution with faster convergence compared to PSO and WHO.

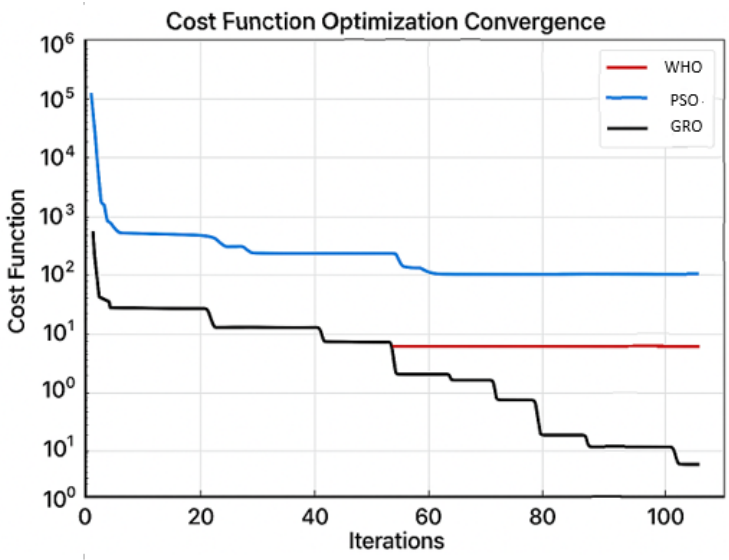

Fig. 8. Cost function of the applied three optimizers

4. Simulated Results

The MATLAB/Simulink simulation platform is used to thoroughly simulate and analyze the GC-PV power plant. The GRO is used to optimize the parameters of the PI control strategy, which is incorporated into the system design to obtain improved control performance. The goal of this improvement is to improve the PV-DCBVS performance under different fault types. To assess the system's dynamic responsiveness, stability, and power quality during grid disruptions, extensive time-domain simulations are conducted under STC.

4.1. Case 1: 3LG fault

The GRO- PI controller is tested under a 3LG fault applied at 3.1 s and cleared at 3.2 s. Results are compared with WOA- PI and PSO- PI to verify the GRO impact. The V-dip (reaches zero) triggers the inverter to supply Q for grid stabilization. Fig. 9 shows stable VDC performance, and Table 3 summarizes key metrics—overshoot, settling time, and steady-state error. The GRO method achieves lower overshoot, faster settling, and smaller steady-state error, demonstrating improved transient response.

Table 3. OS, ST, and PE in case (3LG)

VDC	PSO	WHO	GRO (proposed)
OS (%)	60.45	59.29	57.52
ST (s)	1.089	1.087	1.057
PE (%)	≈0.18	≈0.007	≈0.0017

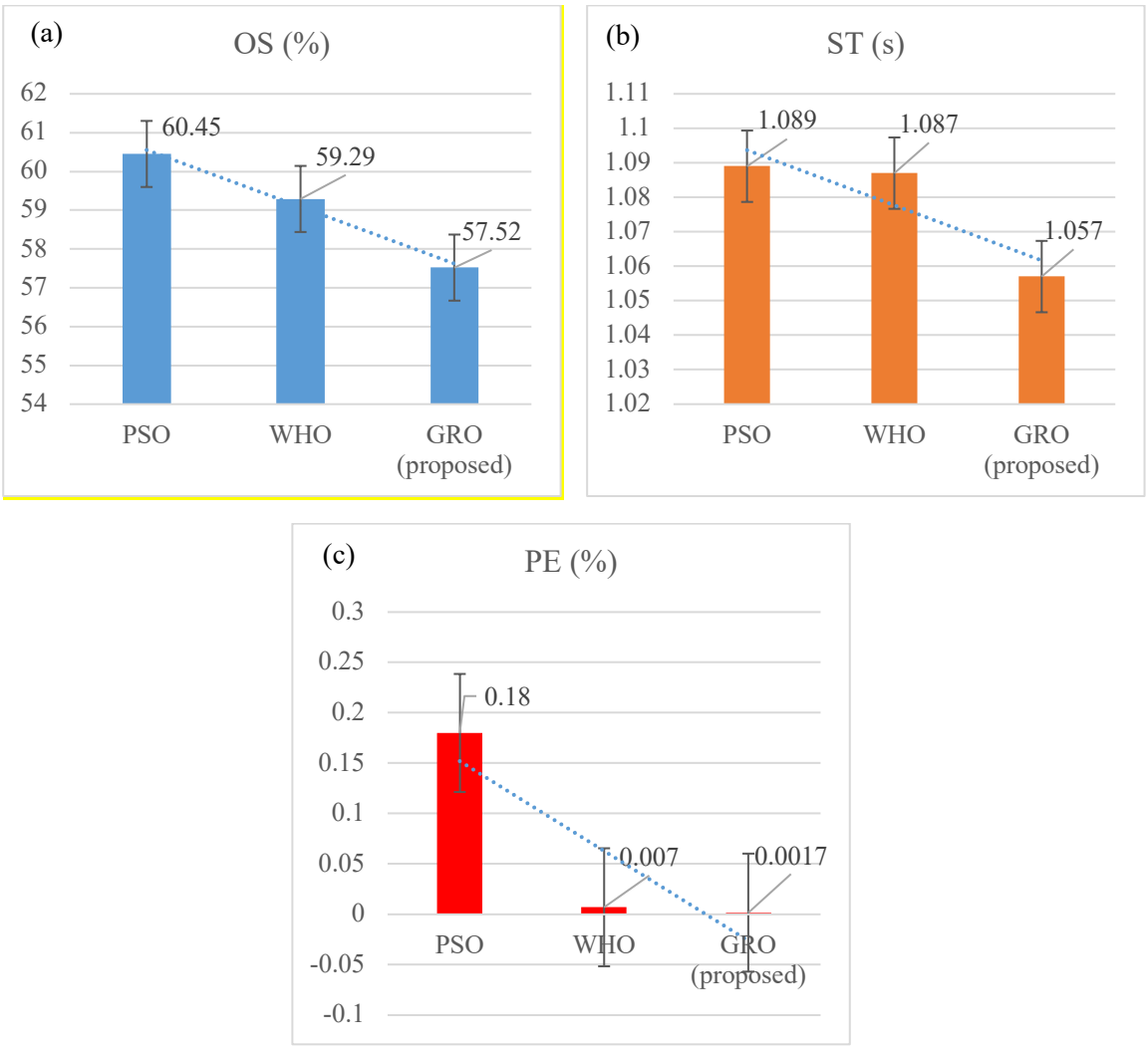

Fig. 9. The VDC key indicators under 3LG fault: (a) OS; (b) ST; (c) PE

4.2. Case 2: 1LG fault

The GRO control method was evaluated for VDC durability under the 1L_G condition. As shown in Table 4, GRO outperforms the others by maintaining an optimal balance between fast transient response and low PE. Although PSO achieved the best VDC regulation, it lagged in other aspects, while WHO exhibited the slowest ST and highest OS as depicted in Fig. 10.

Table 4. OS, ST, and PE in case (1LG)

VDC	PSO	WHO	GRO (proposed)
OS (%)	3.64	5.21	4.57
ST (s)	0.90	0.998	0.917
PE (%)	≈0	≈0.06	≈0.007

4.3. Case 3: 2LG fault

Under the 2L_G condition (Table 5, Fig. 11), GRO again delivers the most balanced performance, combining quick settling with high accuracy. WOA achieves the lowest PE but slower dynamics, whereas PSO shows higher OS and reduced stability.

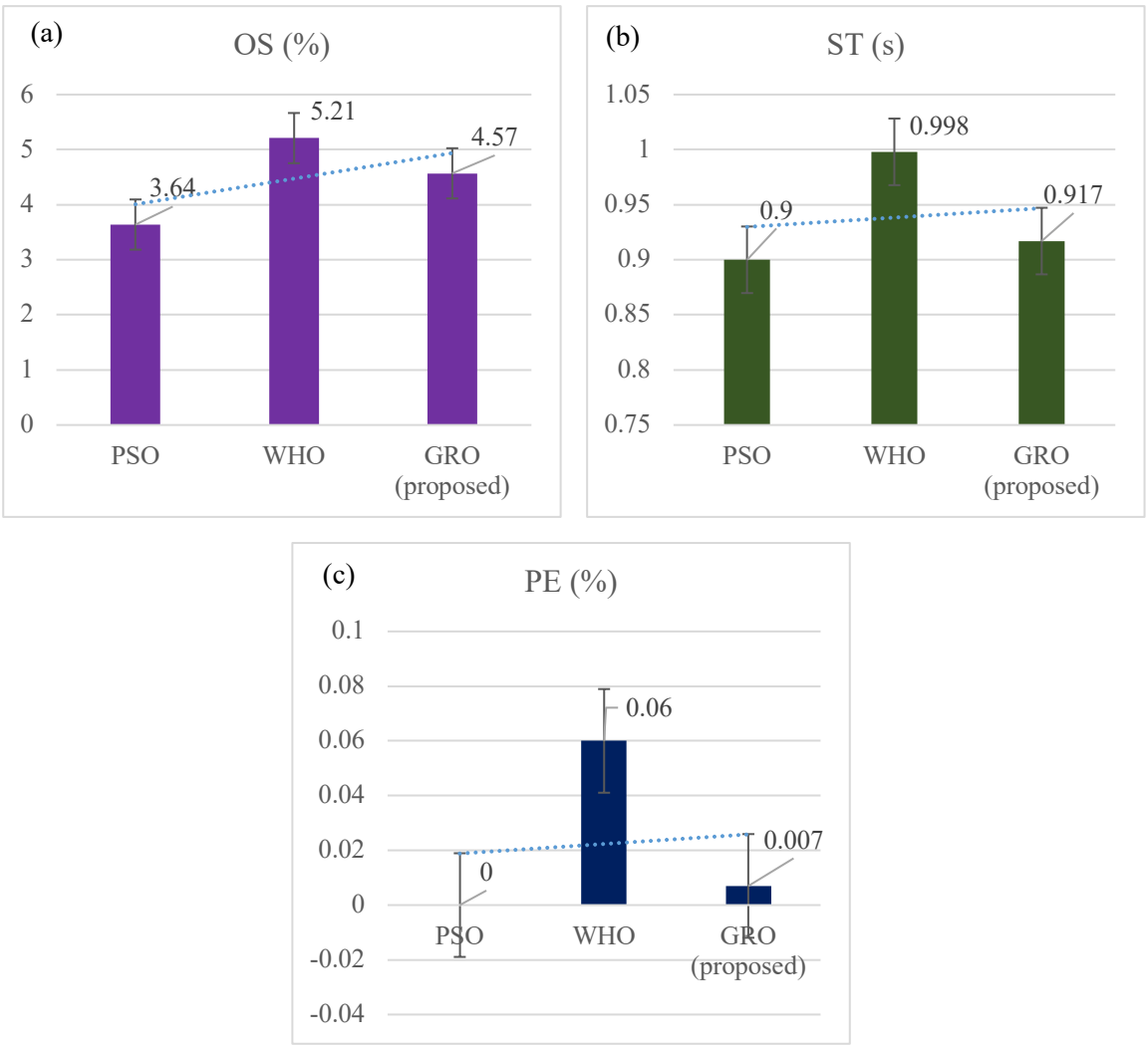

Fig. 10. The VDC key indicators under 1LG fault: (a) OS; (b) ST; (C) PE

Table 5. OS, ST, and PE in case (2LG)

VDC	PSO	WHO	GRO (proposed)
OS (%)	23.54	23.62	22.89
ST (s)	0.97	1.02	0.94
PE (%)	≈0.03	≈0.004	≈0.001

4.4. Case 4: 2L fault

For the line-to-line (L_L) fault case (Table 6, Fig. 12), GRO remains the most consistent approach, providing a good trade-off between speed and precision. WOA offers high accuracy but slower recovery, and PSO responds faster but with greater overshoot. Overall, GRO demonstrates the best compromise between transient and steady-state performance across all fault scenarios.

Table 6. OS, ST, and PE in case (2L)

VDC	PSO	WHO	GRO (proposed)
OS (%)	18.48	18.78	17.73
ST (s)	0.947	1.013	0.923
PE (%)	≈0.02	≈0.002	≈0.001

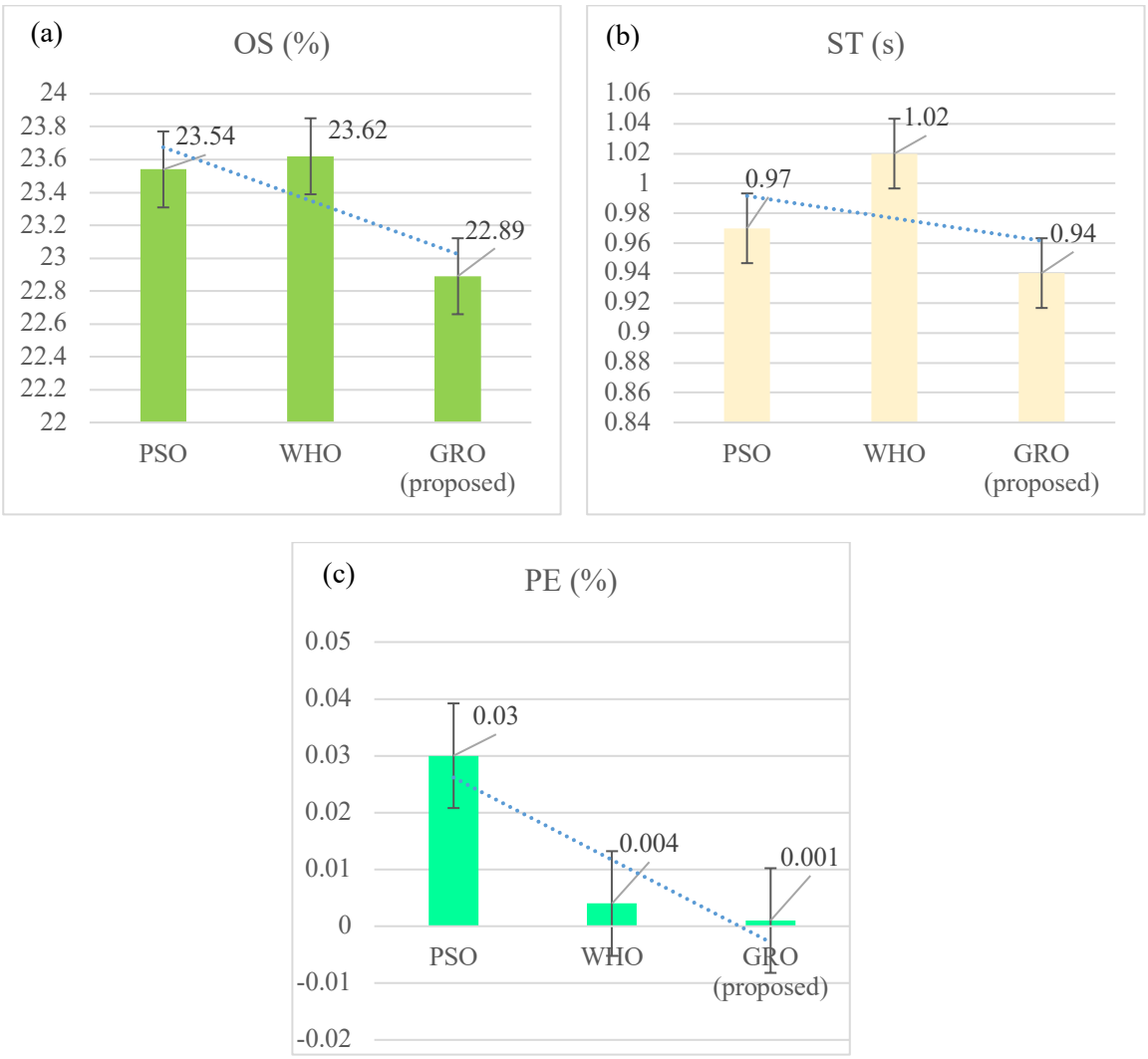

Fig. 11. The VDC key indicators under 2LG fault: (a) OS; (b) ST; (C) PE

5. Discussions

The VDC performance of the GC- PV system was analyzed using three optimization techniques: PSO, WHO, and the proposed GRO. The comparison, based on OS, ST, and PE, consistently shows that the proposed GRO method achieves superior overall performance. For various operating conditions, GRO provides smoother transient behavior, faster settling, and higher voltage accuracy than PSO and WHO. For instance, GRO achieves the lowest OS values of 57.52%, 22.89%, 17.73%, and 4.57% across different test scenarios, indicating reduced voltage stress and improved transient stability as seen in Fig. 13. It also demonstrates the fastest STs of 1.057 s, 0.94 s, 0.923 s, and 0.917 s, compared with longer stabilization periods under PSO and WHO as seen in Fig. 14. Moreover, the GRO controller achieves exceptionally low PEs—approximately 0.0017%, 0.001%, 0.001%, and 0.007%—highlighting its superior precision in maintaining the reference VDC as seen in Fig. 15. Overall, the proposed GRO-based controller offers enhanced voltage regulation, faster dynamic response, and better steady-state accuracy, ensuring more stable and efficient operation of GC-PV systems under varying conditions.

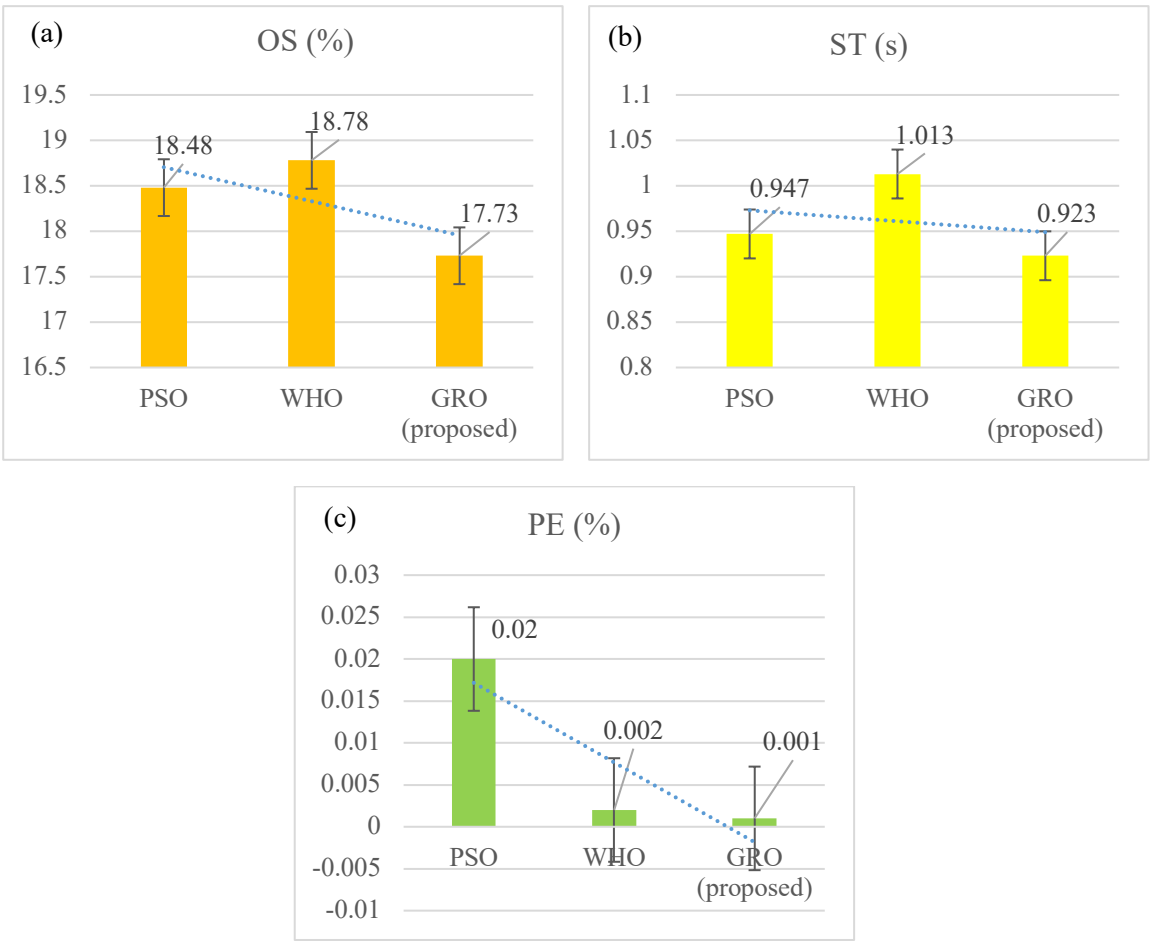

Fig. 12. The VDC key indicators under 2L fault: (a) OS; (b) ST; (C) PE

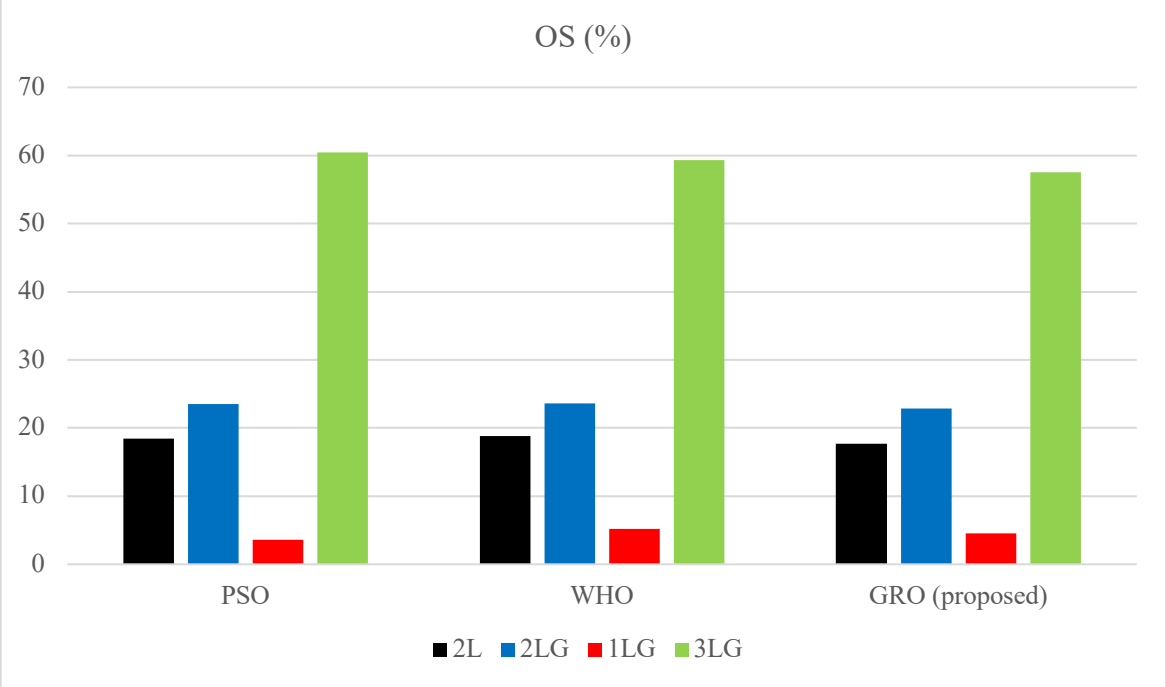

Fig. 13. The OS percentage with the investigated optimizers under the four fault conditions

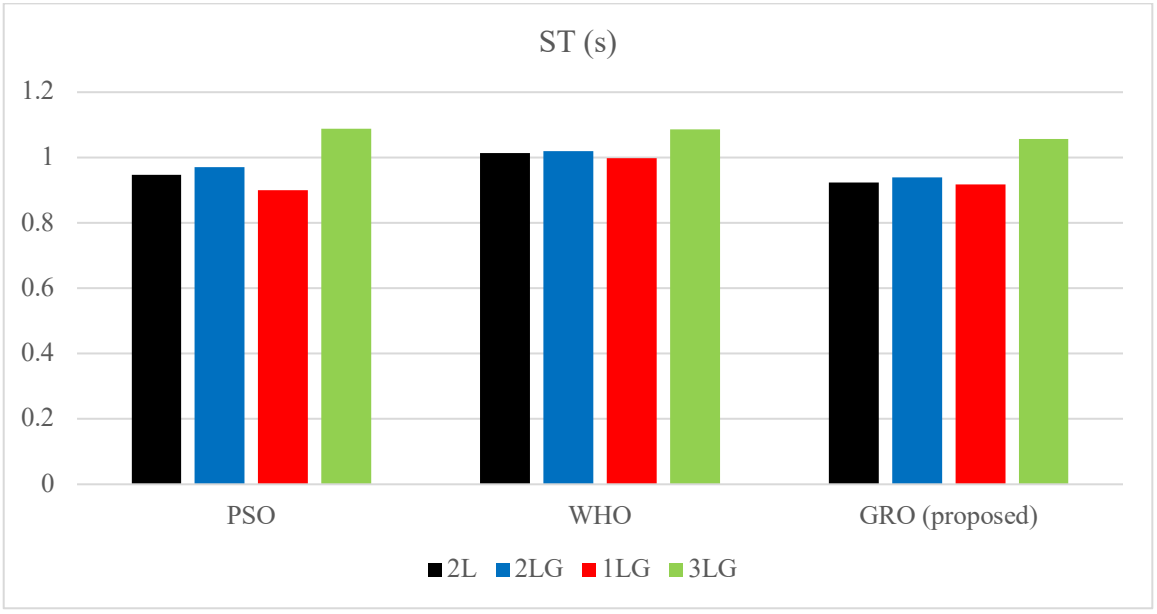

Fig. 14. The ST period with the investigated optimizers under the four fault conditions

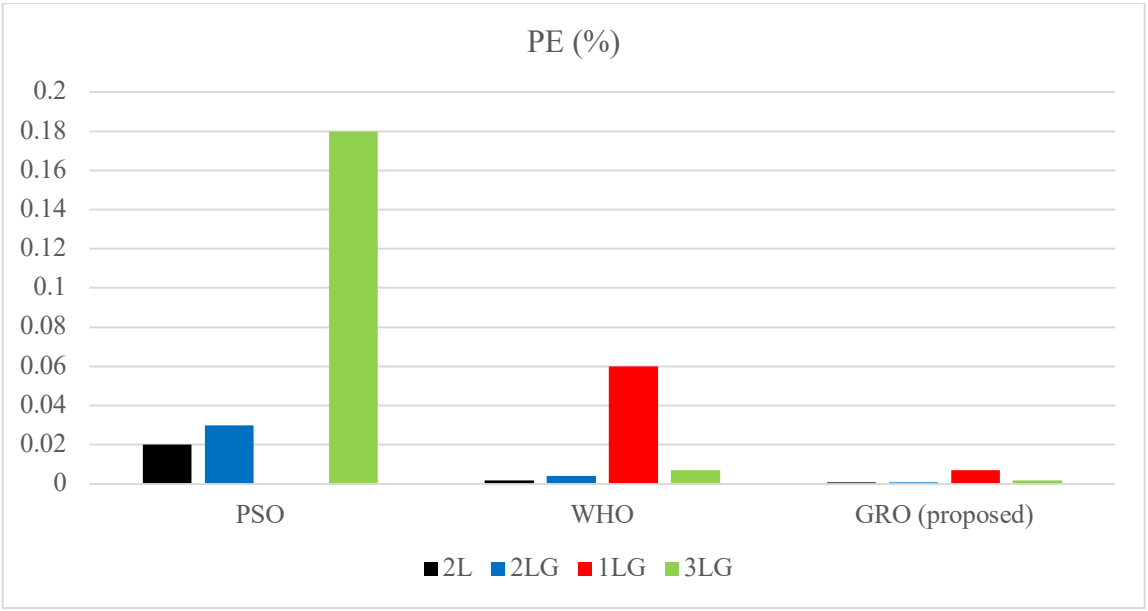

Fig. 15. The PE percentage with the investigated optimizers under the four fault conditions

6. Conclusion

The study verified the effectiveness of the GRO in enhancing the DCBNS of GC- PV systems. By optimally tuning the PI controller, GRO improved both transient and steady-state performance under different fault conditions, outperforming PSO and WOA. In the (3LG, 1L_G, 2L_G, and L_L) fault, it achieved superior VDC stability with minimal overshoot and faster recovery. GRO maintained balanced transient and steady-state responses. GRO achieved quicker voltage recovery and smaller DC-link overshoot, confirming its robustness against grid disturbances. Overall, the GRO method enhanced VDC recovery, minimized oscillations, and maintained grid stability—demonstrating its value for DCBVS in PV plants. Future work should include hardware-in-the-loop testing and potential integration with AI or adaptive control to validate and extend its real-world applicability.

List of Abbreviations

PV: photovoltaic	PI: Proportional-integral
GRO: Gold Rush Optimization	DCBVS: DC bus voltage stability
WHO: Whale Optimization Algorithm	OS: overshoot
PSO: Particle Swarm Optimization	ST: Settling time
VDC: DC-link voltage	SSE: Steady-state error
3L-G: Three-line-to-ground	FFs: Fossil fuels
RESs: Renewable energy sources	GC: Grid-connected
WTs: Wind turbines	FRT: Fault ride through
POA: Pelican optimization algorithm	HAS: Harmony search algorithm
BFO: Bacterial foraging optimization	GA: Genetic algorithm
MPA: Marine Predator Algorithm	GWO: Grey Wolf Optimization
I-V: Current-voltage	SDM: Single-diode model
N_{Series}: Number of modules in series	$N_{Parralel}$: Number of modules in parallel
TC: Triangular carrier	D: Duty cycle
INC: Incremental conductance	PLL: Phase-locked loop
3Ø: Three phases	I: Current
V: Voltage	ISE: Integral of squared error
STC: Standard test conditions	OS: Overshoot
PE: Percentage error	ST: Settling time

Author Contribution: All authors contributed equally to the main contributor to this paper. All authors read and approved the final paper.

Sustainable Development Goals: Sustainable Development Goals mapped to this document, Affordable and Clean Energy Goal 7.

Data Availability: The data used to support the findings of this study are available at reasonable request from the corresponding author.

Conflicts of Interest: The authors declare that they have no conflicts of interest.

Acknowledgment: The authors extend their appreciation to Prince Sattam bin Abdulaziz University for funding this research work through the project number (PSAU/2024/01/31874).

Funding: The authors extend their appreciation to Prince Sattam bin Abdulaziz University for funding this research work through the project number (PSAU/2024/01/31874).

References

[1] W. F. Mbasso, A. Harrison, I. Dagal, M. Metwally Mahmoud, M. Suhail Shaikh, P. Jangir, H. Kotb, A. Smerat, M. Khishe, and R. Kumar, "Policy-driven expansion of renewable energy in Cameroon: A technical and sustainability-centered analysis of growth trends and cross-sectoral impacts (2015–2024)," *Energy Strategy Reviews*, vol. 62, p. 101912, 2025, https://doi.org/10.1016/j.esr.2025.101912.

[2] A. Hysa, S. Sefa, I. M. Elzein, A. Ma'arif, M. M. Mahmoud, E. Touti, A. M. El-Rifaie, and N. Anwer, "Advanced modeling and comparative error analysis of photovoltaic cells using multi-diode models and EQE characterization," *Journal of Robotics and Control*, vol. 6, no. 5, pp. 2308-2321, Sep. 2025, https://doi.org/10.18196/jrc.v6i5.27539.

[3] D. Cui, A. Harrison, E. Fendzi-Donfack, I. Dagal, P. Jangir, M. Metwally Mahmoud, P. Malkani, W. F. Mbasso, P. Tiako, and A. Smerat, "Enhancing short-term electricity forecasting with advanced machine learning techniques," *Journal of Electrical Engineering & Technology*, Sep. 2025, https://doi.org/10.1007/s42835-025-02430-z.

[4] N. V. A. Ravikumar, R. Sasidhar, V. Manoj, C. Mutta, M. C. S. Reddy, K. Jagath Narayana, D. E. M. Wapet, and M. Metwally Mahmoud, "Design and real-time simulations of robust controllers for uncertain

multi-input wind turbine," *Energy Exploration & Exploitation*, 2025, https://doi.org/10.1177/01445987251373101.

[5] Y. Maamar, I. M. Elzein, A. Benameur, H. Mohamed, M. M. Mahmoud, M. I. Mosaad, and S. A. Shaaban, "A comparative analysis of recent MPPT algorithms (P&O / INC / FLC) for PV systems," *Journal of Robotics and Control*, vol. 6, no. 4, pp. 1581-1588, 2025, https://doi.org/10.18196/jrc.v6i4.25814.

[6] S. Basu, M. Basu, C. Jena, I. M. Elzein, W. F. Mbasso, M. Metwally Mahmoud, A. Ma'arif, K. A. Metwally, and S. A. Shaaban, "Applications of snow ablation optimizer for sustainable dynamic dispatch of power and natural gas assimilating multiple clean energy sources," *Engineering Reports*, vol. 7, no. 6, p. e70211, 2025, https://doi.org/10.1002/eng2.70211.

[7] N. F. Ibrahim, M. M. Mahmoud, A. M. H. Al Thaiban, A. B. Barnawi, Z. M. S. Elbarbary, A. I. Omar, and H. Abdelfattah, "Operation of grid-connected PV system with ANN-based MPPT and an optimized LCL filter using GRG algorithm for enhanced power quality," *IEEE Access*, vol. 11, pp. 106859–106876, 2023, https://doi.org/10.1109/ACCESS.2023.3317980.

[8] I. El Maysse, A. El Magri, A. Watil, A. Alkuhayli, M. Kissaoui, R. Lajouad, F. Giri, and M. Metwally Mahmoud, "Nonlinear observer-based controller design for VSC-based HVDC transmission systems under uncertainties," *IEEE Access*, vol. 11, pp. 124014–124030, 2023, https://doi.org/10.1109/ACCESS.2023.3330440.

[9] S. Heroual, B. Belabbas, I. M. Elzein, Y. Diab, A. Ma'arif, M. Mahmoud, T. Allaoui, and N. Benabdallah, "Enhancement of transient stability and power quality in grid-connected PV systems using SMES," *International Journal of Robotics and Control Systems*, vol. 5, no. 2, pp. 990–1005, 2025, https://doi.org/10.31763/ijrcs.v5i2.1760.

[10] N. F. Ibrahim, M. M. Mahmoud, H. Alnami, D. E. M. Wapet, S. A. E. M. Ardjoun, M. I. Mosaad, A. M. Hassan, and H. Abdelfattah, "A new adaptive MPPT technique using an improved INC algorithm supported by fuzzy self-tuning controller for a grid-linked photovoltaic system," *PLOS ONE*, vol. 18, no. 11, p. e0293613, Nov. 2023, https://doi.org/10.1371/journal.pone.0293613.

[11] M. Arunadevi, B. Karthikeyan, A. Shrihari, S. Saravanan, K. Sundararaju, R. Palanisamy, M. Awad, M. M. Mahmoud, D. E. M. Wapet, A. A. Al Ayidh, H. S. Hussein, M. M. Hussein, and A. I. Omar, "Prediction of optimum operating parameters to enhance the performance of PEMFC using machine learning algorithms," *Energy Exploration & Exploitation*, vol. 43, no. 2, pp. 676–698, 2025, https://doi.org/10.1177/01445987241290535.

[12] A. Hysa, M. M. Mahmoud, and A. Ewais, "An investigation of the output characteristics of photovoltaic cells using iterative techniques and MATLAB® 2024a software," *Control Systems Optimization Letters*, vol. 3, no. 1, pp. 46–52, 2025, https://doi.org/10.59247/csol.v3i1.174.

[13] M. M. Mahmoud, Y. M. Esmail, B. S. Atia, O. M. Kamel, K. M. AboRas, M. Bajaj, S. S. H. Bukhari, and D. E. M. Wapet, "Voltage quality enhancement of low-voltage smart distribution system using robust and optimized DVR controllers: Application of the Harris Hawks algorithm," *International Transactions on Electrical Energy Systems*, vol. 2022, no. 1, p. 4242996, 2022, https://doi.org/10.1155/2022/4242996.

[14] O. Makram Kamel, I. M. Elzein, M. M. Mahmoud, A. Y. Abdelaziz, M. M. Hussein, and A. A. Zaki Diab, "Effective energy management strategy with a novel design of fuzzy logic and JAYA-based controllers in isolated DC/AC microgrids: A comparative analysis," *Wind Engineering*, vol. 49, no. 1, pp. 199–222, 2025, https://doi.org/10.1177/0309524X241263518.

[15] S. Nadweh, I. M. Elzein, D. E. Mbadjoun Wapet, and M. M. Mahmoud, "Optimizing control of single-ended primary inductor converter integrated with microinverter for PV systems: Imperialist competitive algorithm," *Energy Exploration & Exploitation*, 2025, https://doi.org/10.1177/01445987251382002.

[16] S. Heroual, B. Belabbas, Y. Diab, M. M. Mahmoud, T. Allaoui, and N. Benabdallah, "Optimizing power flow in photovoltaic-hybrid energy storage systems: A PSO and DPSO approach for PI controller tuning," *International Transactions on Electrical Energy Systems*, vol. 2025, no. 1, pp. 1-23, 2025, https://doi.org/10.1155/etep/9958218.

[17] P. Sinha, K. Paul, A. Mohanty, I. M. Elzein, C. S. Mishra, M. M. Mahmoud, D. E. M. Wapet, A. Al Ayidh, A. Althobaiti, H. S. Hussein, T. A. H. Alghamdi, and A. M. Ewais, "Efficient automated detection of power quality disturbances using nonsubsampled contourlet transform & PCA-SVM," *Energy Exploration & Exploitation*, vol. 43, no. 3, pp. 1149–1179, 2025, https://doi.org/10.1177/01445987241312755.

[18] N. F. Ibrahim, S. A. E. M. Ardjoun, M. Alharbi, A. Alkuhayli, M. Abuagreb, U. Khaled, and M. M. Mahmoud, "Multiport converter utility interface with a high-frequency link for interfacing clean energy sources (PV/Wind/Fuel Cell) and battery to the power system: Application of the HHA algorithm," *Sustainability*, vol. 15, no. 18, p. 13716, 2023, https://doi.org/10.3390/su151813716.

[19] F. Menzri, T. Boutabba, I. Benlaloui, H. Bawayan, M. I. Mosaad, and M. M. Mahmoud, "Applications of hybrid SMC and FLC for augmentation of MPPT method in a wind-PV-battery configuration," *Wind Engineering*, vol. 48, no. 6, pp. 1186–1202, 2024, https://doi.org/10.1177/0309524X241254364.

[20] T. Li, H. Fan, S. Zeng, X. Hu, Z. Meng, and Y. Zhao, "A low voltage ride-through strategy for grid-connected PV converters based on variable power point tracking method," *Energy Reports*, vol. 8, pp. 398–404, 2022, https://doi.org/10.1016/j.egyr.2022.08.167.

[21] S. R. K. Joga, P. Sinha, V. Manoj, S. R. Sura, V. N. Pudi, N. F. Ibrahim, A. Alkuhayli, M. M. Hussein, U. Khaled, D. E. M. Wapet, A. Beroual, and M. M. Mahmoud, "Applications of tunable-Q factor wavelet transform and AdaBoost classifier for identification of high impedance faults: Towards the reliability of electrical distribution systems," *Energy Exploration & Exploitation*, vol. 42, no. 6, pp. 2017–2055, 2024, https://doi.org/10.1177/01445987241260949.

[22] R. Rai and B. Singh, "Converter control during low voltage ride through operation for grid-interfaced solar PV battery assisted system," *IEEE Transactions on Industrial Electronics*, vol. 70, no. 9, pp. 9181–9191, 2023, https://doi.org/10.1109/TIE.2022.3213900.

[23] A. Khan, M. M. Khan, Z. Uddin, J. Chuanwen, and A. Y. Abdelaziz, "Grid-interfaced photovoltaic system with enhanced resilient control schemes for low-voltage ride-through," *Electrical Engineering*, vol. 106, no. 1, pp. 773–792, 2024, https://doi.org/10.1007/s00202-023-01994-1.

[24] S. Bagchi, D. Chatterjee, R. Bhaduri, and P. K. Biswas, "An improved low-voltage ride-through (LVRT) strategy for PV-based grid-connected inverter using instantaneous power theory," *IET Generation Transmission & Distribution*, vol. 15, no. 5, pp. 883–893, 2021, https://doi.org/10.1049/gtd2.12066.

[25] A. K. Singh, D. K. Tiwari, N. B. D. Choudhury, and J. Singh, "A multi-objective low-voltage ride-through control strategy for three-phase grid-interfaced solar power plant during symmetrical and asymmetrical faults," *International Journal of Circuit Theory and Applications*, vol. 52, no. 9, pp. 4399–4420, 2024, https://doi.org/10.1002/cta.3976.

[26] S. Basu Roy Chowdhury and P. K. Gayen, "An improved capability of LVRT in single-stage three-phase grid-linked PV systems," *Electrical Engineering*, vol. 106, no. 1, pp. 125–143, 2024, https://doi.org/10.1007/s00202-023-01968-3.

[27] G. Yang, J. Zhang, H. Zhang, C. Wang, Y. Zhu, and X. Chen, "Impact of large-scale photovoltaic-energy storage power generation system access on differential protection of main transformer under symmetrical faults," *Frontiers in Energy Research*, vol. 11, pp. 1-13, 2023, https://doi.org/10.3389/fenrg.2023.1115110.

[28] D. J. Rincon, M. A. Mantilla, J. M. Rey, M. Garnica, and D. Guilbert, "An overview of flexible current control strategies applied to LVRT capability for grid-connected inverters," *Energies*, vol. 16, no. 3, p. 1052, 2023, https://doi.org/10.3390/en16031052.

[29] J. Joshi, A. K. Swami, V. Jately, and B. Azzopardi, "A comprehensive review of control strategies to overcome challenges during LVRT in PV systems," *IEEE Access*, vol. 9, pp. 121804–121834, 2021, https://doi.org/10.1109/ACCESS.2021.3109050.

[30] S. Wang, X. Tang, X. Liu, and C. Xu, "Research on low voltage ride through control of a marine photovoltaic grid-connected system based on a super capacitor," *Energies*, vol. 15, no. 3, p. 1020, 2022, https://doi.org/10.3390/en15031020.

[31] H. Boudjemai, S. A. E. M. Ardjoun, H. Chafouk, M. Denai, M. Aljohani, M. I. Mosaad, and M. M. Mahmoud, "Design, simulation, and experimental validation of a new fuzzy logic-based maximal power point tracking strategy for low power wind turbines," *International Journal of Fuzzy Systems*, vol. 26, no. 8, pp. 2567–2584, 2024, https://doi.org/10.1007/s40815-024-01747-7.

[32] M. A. Shawqi, M. H. Abdallah, and I. A. Nassar, "Impact of on-grid solar energy generation system on low voltage ride through capability," *International Journal of Power Electronics and Drive Systems*, vol. 13, no. 1, pp. 488–499, 2022, https://doi.org/10.11591/ijpeds.v13.i1.pp488-499.

[33] H. Zahloul, A. Khaliq, H. Hamzehbahmani, S. Veremieiev, and S. Salous, "Evaluation of LVRT capability and stability analysis of VSC-based advanced control approach for grid-connected PV system under grid fault conditions," *Heliyon*, vol. 10, no. 5, pp. 1-18, 2024, https://doi.org/10.1016/j.heliyon.2024.e26935.

[34] K. Zeb, S. U. Islam, I. Khan, W. Uddin, M. Ishfaq, T. D. C. Busarello, S. M. Muyeen, I. Ahmad, and H. J. Kim, "Faults and fault ride through strategies for grid-connected photovoltaic system: A comprehensive review," *Renewable and Sustainable Energy Reviews*, vol. 158, p. 112125, 2022, https://doi.org/10.1016/j.rser.2022.112125.

[35] R. Kassem, M. M. Mahmoud, N. F. Ibrahim, A. Alkuhayli, U. Khaled, A. Beroual, and H. Saleeb, "A techno-economic-environmental feasibility study of residential solar photovoltaic/biomass power generation for rural electrification: A real case study," *Sustainability*, vol. 16, no. 5, p. 2036, 2024, https://doi.org/10.3390/su16052036.

[36] T. N. L. Vu, V. L. Chuong, N. T. N. Truong, and J. H. Jung, "Analytical design of fractional-order PI controller for parallel cascade control systems," *Applied Sciences*, vol. 12, no. 4, p. 2222, 2022, https://doi.org/10.3390/app12042222.

[37] E. Çelik, N. Öztürk, and E. H. Houssein, "Influence of energy storage device on load frequency control of an interconnected dual-area thermal and solar photovoltaic power system," *Neural Computing and Applications*, vol. 34, no. 22, pp. 20083–20099, 2022, https://doi.org/10.1007/s00521-022-07558-x.

[38] S. A. Mohamed, N. Anwer, and M. M. Mahmoud, "Solving optimal power flow problem for IEEE-30 bus system using a developed particle swarm optimization method: Towards fuel cost minimization," *International Journal of Modelling and Simulation*, vol. 45, no. 1, pp. 307–320, 2025, https://doi.org/10.1080/02286203.2023.2201043.

[39] B. K. Ponukumati, P. Sinha, K. Paul, D. E. Mbadjoun Wapet, H. S. Hussein, A. M. Hassan, and M. M. Mahmoud, "Evolving fault diagnosis scheme for unbalanced distribution network using fast normalized cross-correlation technique," *PLOS ONE*, vol. 19, no. 10, pp. 1–23, 2024, https://doi.org/10.1371/journal.pone.0305407.

[40] A. Alkuhayli, U. Khaled, and M. M. Mahmoud, "A novel hybrid Harris hawk optimization–sine cosine transmission network," *Energies*, vol. 17, no. 19, p. 4985, 2024, https://doi.org/10.3390/en17194985.

[41] N. Kumari, N. Malik, A. N. Jha, and G. Mallesham, "Design of PI controller for automatic generation control of multi area interconnected power system using bacterial foraging optimization," *International Journal of Engineering and Technology*, vol. 8, no. 6, pp. 2779–2786, 2016, https://doi.org/10.21817/ijet/2016/v8i6/160806236.

[42] H. H. Ellithy, H. M. Hasanien, M. Alharbi, M. A. Sobhy, A. M. Taha, and M. A. Attia, "Marine predator algorithm-based optimal PI controllers for LVRT capability enhancement of grid-connected PV systems," *Biomimetics*, vol. 9, no. 2, p. 66, 2024, https://doi.org/10.3390/biomimetics9020066.

[43] S. Senthilkumar, V. Mohan, S. P. Mangaiyarkarasi, and M. Karthikeyan, "Analysis of single-diode PV model and optimized MPPT model for different environmental conditions," *International Transactions on Electrical Energy Systems*, vol. 2022, no. 1, p. 4980843, 2022, https://doi.org/10.1155/2022/4980843.

[44] H. M. Ridha, H. Hizam, S. Mirjalili, M. L. Othman, M. E. Ya'acob, and L. Abualigah, "A novel theoretical and practical methodology for extracting the parameters of the single and double diode photovoltaic models," *IEEE Access*, vol. 10, pp. 11110–11137, 2022, https://doi.org/10.1109/ACCESS.2022.3142779.

[45] O. S. Elazab, M. Debouza, H. M. Hasanien, S. M. Muyeen, and A. Al-Durra, "Salp swarm algorithm-based optimal control scheme for LVRT capability improvement of grid-connected photovoltaic power plants: Design and experimental validation," *IET Renewable Power Generation*, vol. 14, no. 4, pp. 591–599, 2020, https://doi.org/10.1049/iet-rpg.2019.0726.

[46] S. Ashfaq, I. El Myasse, D. Zhang, A. S. Musleh, B. Liu, A. A. Telba, U. Khaled, and M. M. Mahmoud, "Comparing the role of long duration energy storage technologies for zero-carbon electricity systems," *IEEE Access*, vol. 12, pp. 73169–73186, 2024, https://doi.org/10.1109/ACCESS.2024.3397918.

[47] R. Kassem, N. F. Ibrahim, M. M. Mahmoud, A. Alkuhayli, U. Khaled, A. Beroual, and H. M. I. Saleeb, "Enhanced multiphase interleaved boost converter interface for grid-connected PV power system," *IEEE Access*, vol. 12, pp. 151940–151954, 2024, https://doi.org/10.1109/ACCESS.2024.3469540.

[48] H. M. I. Saleeb, M. M. Mahmoud, N. F. Ibrahim, A. Alkuhayli, U. Khaled, A. Beroual, and R. Kassem, "Highly efficient isolated multiport bidirectional DC/DC converter for PV applications," *IEEE Access*, vol. 12, pp. 114480–114494, 2024, https://doi.org/10.1109/ACCESS.2024.3442711.

[49] N. A. Maged, H. M. Hasanien, and M. Alharbi, "Electric eel foraging algorithm-based optimal control for low voltage ride through capability improvement of grid-connected photovoltaic power plants," *Ain Shams Engineering Journal*, vol. 15, no. 7, p. 102855, 2024, https://doi.org/10.1016/j.asej.2024.102855.

[50] M. Al-Dhaifallah, A. M. Nassef, H. Rezk, and K. S. Nisar, "Optimal parameter design of fractional order control based INC-MPPT for PV system," *Solar Energy*, vol. 159, pp. 650–664, 2018, https://doi.org/10.1016/j.solener.2017.11.040.

[51] A. Fatah, T. Boutabba, I. Benlaloui, S. Drid, M. M. Mahmoud, M. M. Hussein, W. F. Mbasso, H. S. Hussein, and A. M. Ewias, "Design and dynamic evaluation of a novel photovoltaic pumping system emulation with DS1104 hardware setup: Towards innovative in Green Energy Systems," *PLOS ONE*, vol. 19, no. 10, pp. 1–24, 2024, https://doi.org/10.1371/journal.pone.0308212.

[52] F. Menzri, T. Boutabba, I. Benlaloui, L. Chrifi-Alaoui, A. Alkuhayli, U. Khaled, and M. M. Mahmoud, "Applications of novel combined controllers for optimizing grid-connected hybrid renewable energy systems," *Sustainability*, vol. 16, no. 16, p. 6825, 2024, https://doi.org/10.3390/su16166825.

[53] B. S. Atia, M. M. Mahmoud, I. M. Elzein, A.-M. Mohamed Abdel-Rahim, A. Alkuhayli, U. Khaled, A. Beroual, and S. A. Shaaban, "Applications of Kepler algorithm-based controller for DC chopper: Towards stabilizing wind driven PMSGs under nonstandard voltages," *Sustainability*, vol. 16, no. 7, p. 2952, 2024, https://doi.org/10.3390/su16072952.

[54] M. M. Mahmoud, M. M. Aly, and A. M. M. Abdel-Rahim, "Enhancing the dynamic performance of a wind-driven PMSG implementing different optimization techniques," *SN Applied Sciences*, vol. 2, no. 4, p. 684, 2020, https://doi.org/10.1007/s42452-020-2439-3.

[55] M. N. A. Hamid, F. A. Banakhr, T. H. Mohamed, S. M. Ali, M. M. Mahmoud, M. I. Mosaad, A. A. H. Albla, and M. M. Hussein, "Adaptive frequency control of an isolated microgrids implementing different recent optimization techniques," *International Journal of Robotics and Control Systems*, vol. 4, no. 3, pp. 1000–1012, 2024, https://doi.org/10.31763/ijrcs.v4i3.1432.

[56] M. M. Mahmoud, M. M. Aly, H. S. Salama, and A. M. M. Abdel-Rahim, "Dynamic evaluation of optimization techniques-based proportional-integral controller for wind-driven permanent magnet synchronous generator," *Wind Engineering*, vol. 45, no. 3, pp. 696–709, 2021, https://doi.org/10.1177/0309524X20930421.

[57] M. M. Mahmoud, M. K. Ratib, M. M. Aly, and A.-M. M. Abdel-Rahim, "Application of whale optimization technique for evaluating the performance of wind-driven PMSG under harsh operating events," *Process Integration and Optimization for Sustainability*, vol. 6, no. 2, pp. 447–470, 2022, https://doi.org/10.1007/s41660-022-00224-8.

[58] M. M. Hussein, T. H. Mohamed, M. M. Mahmoud, M. Aljohania, M. I. Mosaad, and A. M. Hassan, "Regulation of multi-area power system load frequency in presence of V2G scheme," *PLOS ONE*, vol. 18, no. 9, p. e0291463, 2023, https://doi.org/10.1371/journal.pone.0291463.

[59] A. T. Hassan, F. A. Banakhr, M. M. Mahmoud, M. M. Mosaad, A. F. Rashwan, M. R. Mosa, M. M. Hussein, and T. Mohamed, "Adaptive load frequency control in microgrids considering PV sources and EVs impacts: Applications of hybrid sine cosine optimizer and balloon effect identifier algorithms," *International Journal of Robotics and Control Systems*, vol. 4, no. 2, pp. 941–957, 2024, https://doi.org/10.31763/ijrcs.v4i2.1448.

[60] K. Zolfi, "Gold rush optimizer: A new population-based metaheuristic algorithm," *Operations Research and Decisions*, vol. 33, no. 1, pp. 113–150, 2023, https://doi.org/10.37190/ord230108.

[61] M. Saglam, Y. Bektas, and O. A. Karaman, "Dandelion optimizer and gold rush optimizer algorithm-based optimization of multilevel inverters," *Arabian Journal for Science and Engineering*, vol. 49, no. 5, pp. 7029–7052, 2024, https://doi.org/10.1007/s13369-023-08654-3.

[62] H. H. Ali and A. Fathy, "Reliable exponential distribution optimizer-based methodology for modeling proton exchange membrane fuel cells at different conditions," *Energy*, vol. 292, p. 130600, 2024, https://doi.org/10.1016/j.energy.2024.130600.

[63] O. M. Lamine, N. Bessous, A. Borni, F. A. Banakhr, M. I. Mosaad, O. Mammeri, and M. M. Mahmoud, "A combination of INC and fuzzy logic-based variable step size for enhancing MPPT of PV systems," *International Journal of Robotics and Control Systems*, vol. 4, no. 2, pp. 877–892, 2024, https://doi.org/10.31763/ijrcs.v4i2.1428.

[64] H. Abdelfattah, M. Esmail, S. A. Kotb, M. M. Mahmoud, H. S. Hussein, D. E. M. Wapet, A. I. Omar, and A. M. Ewais, "Optimal controller design for reactor core power stabilization in a pressurized water reactor: Applications of gold rush algorithm," *PLOS ONE*, vol. 19, no. 1, p. e0296987, 2024, https://doi.org/10.1371/journal.pone.0296987.

[65] A. M. Ewias, S. H. Hakmi, T. H. Mohamed, M. M. Mahmoud, A. Eid, A. Y. Abdelaziz, and Y. A. Dahab, "Advanced load frequency control of microgrid using a bat algorithm supported by a balloon effect identifier in the presence of photovoltaic power source," *PLOS ONE*, vol. 18, no. 10, p. e0293246, 2023, https://doi.org/10.1371/journal.pone.0293246.